LAMINAR FLAMELET CONCEPTS IN TURBULENT COMBUSTION

N. PETERS

Institut für Allgemeine Mechanik
RWTH Aachen, West-Germany

The laminar flamelet concept covers a regime in turbulent combustion where chemistry (as compared to transport processes) is fast such that it occurs in asymptotically thin layers—called flamelets—embedded within the turbulent flow field. This situation occurs in most practical combustion systems including reciprocating engines and gas turbine combustors. The inner structure of the flamelets is one-dimensional and time dependent. This is shown by an asymptotic expansion for the Damköhler number of the rate determining reaction which is assumed to be large. Other non-dimensional chemical parameters such as the nondimensional activation energy or Zeldovich number may also be large and may be related to the Damköhler number by a distinguished asymptotic limit. Examples of the flamelet structure are presented using one-step model kinetics or a reduced four-step quasi-global mechanism for methane flames.

For *non-premixed combustion* a formal coordinate transformation using the mixture fraction Z as independent variable leads to a universal description. The instantaneous scalar dissipation rate χ of the conserved scalar Z is identified to represent the diffusion time scale that is compared with the chemical time scale in the definition of the Damköhler number. Flame stretch increases the scalar dissipation rate in a turbulent flow field. If it exceeds a critical value χ_q the diffusion flamelet will extinguish. Considering the probability density distribution of χ, it is shown how local extinction reduces the number of burnable flamelets and thereby the mean reaction rate. Furthermore, local extinction events may interrupt the connection to burnable flamelets which are not yet reached by an ignition source and will therefore not be ignited. This phenomenon, described by percolation theory, is used to derive criteria for the stability of lifted flames. It is shown how values of χ_q obtained from laminar experiments scale with turbulent residence times to describe lift-off of turbulent jet diffusion flames. For non-premixed combustion it is concluded that the outer mixing field—by imposing the scalar dissipation rate—dominates the flamelet behaviour because the flamelet is attached to the surface of stoichiometric mixture. The flamelet response may be two-fold: burning or non-burning quasi-stationary states. This is the reason why classical turbulence models readily can be used in the flamelet regime of non-premixed combustion. The extent to which burnable yet non-burning flamelets and unsteady transition events contribute to the overall statistics in turbulent non-premixed flames needs still to be explored further.

For *premixed combustion* the interaction between flamelets and the outer flow is much stronger because the flame front can propagate normal to itself. The chemical time scale and the thermal diffusivity determine the flame thickness and the flame velocity. The flamelet concept is valid if the flame thickness is smaller than the smallest length scale in the turbulent flow, the Kolmogorov scale. Also, if the turbulence intensity v' is larger than the laminar flame velocity, there is a local interaction between the flame front and the turbulent flow which corrugates the front. A new length scale $L_G = v_F^3/\epsilon$, the Gibson scale, is introduced which describes the smaller size of the burnt gas pockets of the front. Here v_F is the laminar flame velocity and ϵ the dissipation of turbulent kinetic energy in the oncoming flow. Eddies smaller than L_G cannot corrugate the flame front due to their smaller circumferential velocity while larger eddies up to the macro length scale will only convect the front within the flow field.

Flame stretch effects are the most efficient at the smallest scale L_G. If stretch combined with differential diffusion of temperature and the deficient reactant, represented by a Lewis number different from unity, is imposed on the flamelet, its inner structure will respond leading to a change in flame velocity and in some cases to extinction. Transient effects of this response are much more important than for diffusion flamelets. A new mechanism of premixed flamelet extinction, based on the diffusion of radicals out of the reaction zone, is described by Rogg. Recent progress in the Bray-Moss-Libby formulation and the pdf-transport equation approach by Pope are presented. Finally, different approaches to predict the turbulent flame velocity including an argument based on the fractal dimension of the flame front are discussed.

1. Introduction

Turbulent flows with combustion fall essentially into two categories: premixed and non-premixed combustion. Combustion in spark ignition engine occurs in the premixed mode while non-premixed combustion is desirable—for safety reasons—in furnaces, Diesel engines and in gas turbine combustion chambers. The two categories also are different from a fundamental point of view as far as the different time scales for convection, diffusion and reaction are concerned. Premixing prior to combustion eliminates the diffusion process between fuel and oxidizer as a possible rate limiting step. Nevertheless, diffusion and heat conduction remain important within the flamelet structure of both, premixed and diffusion flames. It may even be shown that convection is a lower order term in the chemically reacting part of flamelets as long as they are asymptotically thin. This is the most fundamental property of a flamelet and will therefore be discussed in the following.

1.1 The flamelet as an asymptotic concept

If the relevant chemical time scale is short compared to the convection and diffusion time scales, combustion takes place within asymptotically thin layers embedded in the turbulent flow. These layers, which have a well defined inner structure, now are called flamelets*). The asymptotic procedure is similar to that initiated by Prandtl[1] in 1904 for boundary layers. Zel'dovich and Frank-Kamenetskii[2] in 1938 were the first to use asymptotic reasoning in flame theory, but it took until 1961 for a systematic asymptotic description of the inner diffusion flame structure by Liñán[3] and until 1969 for that of a premixed flame by Bush and Fendell[4].

In order to locate a flamelet in a turbulent flow it is useful to introduce a coordinate system that is attached to the flamelet structure. Thereby the influence of external parameters on the flamelet and its response can be quantified. This was first done by Clavin and Williams[5] for premixed flames and in ref. 6 for diffusion flames. All the work in refs. 2–6 used a one-step reaction model with a large Damköhler number (ref. 3) or a large activation energy (refs. 2, 4–6). Summaries of work based on matched asymptotic expansions in flame theory are given in the recent books by Buckmaster and Ludford[7] and Williams[8].

Real chemistry is, of course, more complicated and the question arises whether flamelets can also be defined for detailed elementary mechanisms. There has been considerable progress over the last decade in predicting the structure of one-dimensional steady flames by numerical methods (Warnatz[9,10], Westbrook and Dryer[11], Dixon-Lewis et al.[12], cf. also refs. 13–14, where further references are given). Numerically, it has been shown that lean and rich hydrogen flames respond to flame stretch in a very similar way as one-step model flames[15]. But only recently the gap between the numerical and asymptotic approach was closed for hydrocarbon flames by a systematic reduction of the elementary kinetic mechanism to four quasi-global steps[16,17]. In this review the asymptotic structure of methane flames will also be discussed in the context of the flamelet concept.

An immediate choice for a large number in an asymptotic expansion is the Damköhler number of the second kind, which is the ratio of the diffusion time scale to the reaction time scale. It is expected to be large if the flamelet is to be thin. In one-step large activation energy asymptotics the Damköhler number (equivalent to the flame speed eigenvalue in premixed flames) is related to the activation energy by a distinguished asymptotic limit[18,19]. This means that, as the non-dimensional activation energy (now called the Zeldovich number[8]) tends to infinity, the Damköhler number must also tend to infinity in a very specific way. For the asymptotic description of the reduced four-step mechanism it can be shown that none of the activation energies plays the role of an expansion parameter and that the overall thickness of the reaction zone is governed by the Damköhler number of the chain breaking reaction H + O_2 + M→HO_2 + M. This reaction is the slowest and therefore rate determining step for the burnout of H_2 and CO. Therefore again, by requiring that the Damköhler number of this reaction is large, a flamelet can be defined as an asymptotic concept.

1.2 Why do classical turbulence models fail in the flamelet regime and what can be done?

In classical turbulence models, equations for the moments of the dependent variables are derived on the basis of the general balance equations. Then it is shown that the hierarchy of equations cannot be closed at any level and empirical closure assumptions are introduced. These assumptions require that the discarded higher moments can be related in a specific and universal way to the lower moments. This is by no means evident, if additional time and

---

*) This definition differs from that of a flame-sheet which is an infinitely thin sheet without a defined inner structure.

length scales due to chemistry determine the general solution. One may therefore want to avoid the description by moments and turn to the most general probabilistic description of a turbulent reacting flow which is contained in the joint probability density function of all dependent variables, i.e. the three velocity components, the temperature and the concentrations. In principle, this pdf could be calculated at each location within the flow field on the basis of a pdf transport equation. Although this approach avoids some of the modelling assumptions used in moment methods and therefore should yield more general results, it still requires modelling of some of the most important terms, in particular the fluctuating pressure gradient term and the molecular diffusion term. A recent review on pdf methods for turbulent reactive flow has been given by Pope[20]. The classical argument to support pdf transport modelling for reactive flows has always been that the highly nonlinear chemical source term does not need to be modelled. However, if reaction occurs in thin layers only, reaction and molecular diffusion are closely coupled and the difficulty with the chemical source term is shifted towards modelling of the molecular diffusion term. In a very interesting pdf-calculation Pope and Anand[21] use the sum of the reaction and diffusion term as appropriate source term for the flamelet regime of premixed flames and compare the results with the standard modelling, which they call the regime of distributed combustion. This paper will also be discussed in section 3.3.

An alternative approach that provides a more direct insight into the physics of the problem is that of a presumed or composite pdf. The idea here is that well defined structures passing over the point of observation should contribute in a quasi-deterministic way to the probability density function. The occurrence of such structures could manifest itself, for example, in a bimodal shape of the pdf. By postulating certain properties of the structure and randomness of the surrounding flow field one can construct a composite pdf which depends on a number of parameters. These can again be related to conditioned and unconditioned moments of the fluctuating variables for which, in principle, moment equations can be derived. An example of a composite pdf for the conserved scalar pdf is given in ref. 22. Here the viscous superlayer between turbulent and non-turbulent fluid was expected to provide a well defined scalar profile. The model was applied by Pitz and Drake[23], Drake, Shyy and Pitz[24] and Chen[25] for diffusion flame studies.

For premixed flames the Bray-Moss-Libby-model presumes the shape of the pdf of the reactive scalar or progress variable to consist essentially of two delta-functions for burnt and unburnt mixtures. This model will be discussed in detail in section 3.3. A presumed beta-function pdf was used in ref. 26 to calculate the mean turbulent reaction rate. The composite or presumed pdf approach leads again to moment equations and is therefore easier to apply than the calculation of the entire pdf.

2. The flamelet concept for non-premixed combustion

Non-premixed combustion is generally associated with diffusion flames which owe their name to the rate controlling step: to diffusion. The convective and diffusive time scales are in general of the same order of magnitude but the chemical time scale is very much smaller. Therefore, the assumption of local chemical equilibrium has been used quite successfully for diffusion flames, in particular those of hydrogen or hydrogen/carbon-monoxide mixtures. The scalar structure that it implies can be thought of as flamelet structure for infinite residence times. For hydrocarbon flames, however, the local equilibrium assumption leads to unrealistically high levels of CO and H_2 on the rich side of the flamelet structure. Many ad-hoc assumptions have been proposed to cure this misbehaviour (cf. Eickhoff[27]). Nevertheless, the important advantage of the local equilibrium assumption is the simplification that it introduces, since it eliminates many parameters— those associated with chemical kinetics—from the analysis.

Non-equilibrium effects are not only important for the prediction of CO, H_2 and also NO_x levels, they also provide the basic mechanism that leads to local quenching of diffusion flamelets and eventually to lift-off and blow-off of jet diffusion flames. A more detailed review of flamelet models in non-premixed combustion was given in ref. 28. Here only the basic features of the analysis will be repeated.

2.1 Introduction of a flame-attached coordinate system

For a two-feed non-premixed system (index 1 denoting the fuel stream and index 2 the oxidizer stream) a fuel element mass fraction Z_F may be defined as the mass fraction of all elements originating from the fuel stream within the mixture. Likewise the oxidizer element mass fraction Z_O is the mass fraction of the

oxygen originating from the oxidizer stream (thereby excluding possible contributions from oxygen contained in the fuel). The fuel as well as the oxidizer stream may contain inerts like nitrogen. Denoting the fuel element mass fraction in the fuel stream by $Z_{F,1}$ equal to $Y_{F,1}$ and the oxygen mass fraction in the oxidizer stream by $Z_{O,2}$ equal to $Y_{O,2}$ the mixture fraction is defined

$$Z = \frac{Z_F}{Z_{F,1}} = 1 - \frac{Z_O}{Z_{O,2}}. \tag{1}$$

The stoichiometric mixture fraction of the reaction

$$\nu_F F + \nu_O O_2 \rightarrow products$$
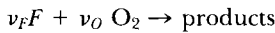
is obtained from $Z_{F,st}/\nu_F M_F = Z_{O,st}/\nu_O M_O$ as

$$Z_{st} = \left[1 + \frac{Y_{F,1} \nu_O M_O}{Y_{O,2} \nu_F M_F}\right]^{-1} \tag{2}$$

and the relation between Z and the equivalence ratio ϕ is given by

$$\phi = \frac{Z}{Z_{st}} \frac{(1-Z_{st})}{(1-Z)} \tag{3}$$

showing that the mixture fraction is uniquely related to the equivalence ratio.

In the balance equation for the mixture fraction the chemical source term cancels identically. If Fick's law for the diffusion flux and equal diffusivities of all species and the temperature are assumed, all Lewis numbers are

$$Le_i = \frac{\lambda}{c_p \rho D_i} = 1 \quad (i = 1, 2, ..., n). \tag{4}$$

Now the balance equations for Z and the temperature T are

$$\rho \frac{\partial Z}{\partial t} + \rho v_\alpha \frac{\partial Z}{\partial x_\alpha} - \frac{\partial}{\partial x_\alpha}\left(\rho D \frac{\partial Z}{\partial x_\alpha}\right) = 0 \tag{5}$$

$$\rho \frac{\partial T}{\partial t} + \rho v_\alpha \frac{\partial T}{\partial x_\alpha} - \frac{\partial}{\partial x_\alpha}\left(\rho D \frac{\partial T}{\partial x_\alpha}\right) = -\frac{1}{c_p} \sum_{i=1}^{n} h_i \dot{m}_i \tag{6}$$

Here h_i are the specific heats and $\dot{m}_i$ the chemical production rates of the reacting species ($i = 1,2,...,n$). The specific heat capacities c_{pi} are all assumed constant and equal to c_p for simplicity. We follow ref. 28 and assume the mixture fraction Z to be given in the flow field as a function of space and time by solution of
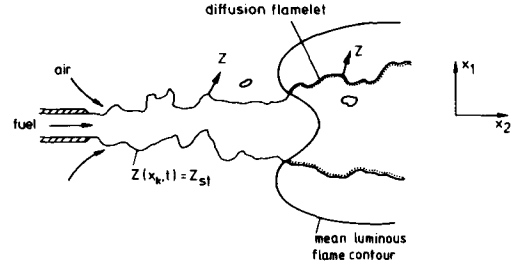

FIG. 1. Schematic illustration of diffusion flamelets attached to the surface of stoichiometric mixture.

eq. (5). Then the surface of stoichiometric mixture can be determined from

$$Z(x_\alpha, t) = Z_{st}. \tag{7}$$

Combustion takes place in a thin layer in the vicinity of this surface if the local mixture fraction gradient is sufficiently high. Let us locally introduce a coordinate system attached to the surface of stoichiometric mixture. We replace the coordinate x_1 by the mixture fraction Z and define the original coordinate system such that the coordinate x_1 does not lie within this surface (cf. Fig. 1). This is a coordinate transformation of the Crocco-type (Crocco expressed the temperature as function of another dependent variable, the velocity, in a flat plate boundary layer). Here the temperature T will be expressed as function of the mixture fraction Z. By definition, the new coordinate Z is locally normal to the surface of stoichiometric mixture. Using $Z_2 = x_2$, $Z_3 = x_3$, $t^* = t$ as the other independent variables, we obtain with the transformation rules

$$\frac{\partial}{\partial t} = \frac{\partial}{\partial t^*} + \frac{\partial Z}{\partial t} \frac{\partial}{\partial Z}, \quad \frac{\partial}{\partial x_1} = \frac{\partial Z}{\partial x_1} \frac{\partial}{\partial Z}$$

$$\frac{\partial}{\partial x_k} = \frac{\partial}{\partial Z_k} + \frac{\partial Z}{\partial x_k} \frac{\partial}{\partial Z}, \quad (k = 2, 3) \tag{8}$$

the temperature equation in the form

$$\rho\left(\frac{\partial T}{\partial t^*} + v_2 \frac{\partial T}{\partial Z_2} + v_3 \frac{\partial T}{\partial Z_3}\right) - \frac{\partial(\rho D)}{\partial x_2} \frac{\partial T}{\partial Z_2}$$

$$- \frac{\partial(\rho D)}{\partial x_3} \frac{\partial T}{\partial Z_3} - \rho D\left[\left(\frac{\partial Z}{\partial x_\alpha}\right)^2 \frac{\partial^2 T}{\partial Z^2} + 2 \frac{\partial Z}{\partial x_2} \frac{\partial^2 T}{\partial Z \partial Z_2}\right.$$

$$\left. + 2 \frac{\partial Z}{\partial x_3} \frac{\partial^2 T}{\partial Z \partial Z_3} + \frac{\partial^2 T}{\partial Z_2^2} + \frac{\partial^2 T}{\partial Z_3^2}\right] = -\frac{1}{c_p} \sum_{i=1}^{n} h_i \dot{m}_i. \tag{9}$$

If the flamelet is thin in the Z-direction, an order of magnitude analysis similar to that for a boundary layer shows that the second deriva-

tive with respect to Z is the dominating term on the left hand side of eq. (9). This term must balance the reaction term on the right hand side. The term containing the time derivative is only important if very rapid changes, such as extinction, occur. Formally this can be shown by introducing the stretched coordinate ζ and the fast time scale τ

$$\zeta = (Z - Z_{st}) / \epsilon \ , \quad \tau = t^*/\epsilon^2 \qquad (10)$$

where ϵ is the inverse of some power of a Damköhler number.

A formal asymptotic description of the flamelet structure for a one-step reaction has been performed in ref. 6 using the results from Liñán's[19] asymptotic analysis of a counter flow diffusion flame. If the time derivative term is retained, the flamelet structure is to leading order described by the one-dimensional time-dependent temperature equation

$$\rho\frac{\partial T}{\partial t} - \rho\frac{\chi_{st}}{2}\frac{\partial^2 T}{\partial Z^2} = -\frac{1}{c_p}\sum_{i=1}^{n} h_i \dot{m}_i. \qquad (11)$$

Similar equations may be derived for the chemical species. In eq.(11)

$$\chi_{st} = 2D_{st}\left(\frac{\partial Z}{\partial x}\right)_{st}^2 \qquad (12)$$

is the instantaneous scalar dissipation rate at stoichiometry. It has the dimension 1/sec and may be interpreted as the inverse of a characteristic diffusion time. Due to the transformation it implicitly incorporates the influence of convection and diffusion normal to the surface of stoichiometric mixture. In ref. 28 the physical significance of χ_{st} has been discussed in detail. In essence, χ_{st} decreases due to diffusion and increases due to straining by the flow field. Chemistry models, including the local equilibrium model and the flame-sheet model in the limit $\chi_{st}\to 0$, have been presented. In ref. 6 it has been shown that local quenching of the flamelet occurs, if χ_{st} exceeds a critical value χ_q. This analysis was based on a one-step-reaction model with a large activation energy. An extension to an one-step reversible reaction is presented in ref. 29. Here we want to discuss the nonequilibrium flamelet structure on the basis of a reduced reaction mechanism for methane flames.
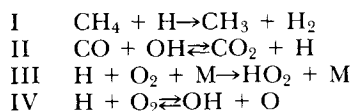
2.2 The inner structure of stretched steady state diffusion flamelets

The one-step mechanism with a large activation energy describes quenching as a thermal effect where heat conduction out of the reaction zone exceeds heat generation due to reaction, which in itself is very sensitive to temperature changes. While this remains to be the basic mechanism for diffusion flame quenching, the details of the flame structure of hydrocarbon flames are not correctly predicted by the one-step mechanism. As Bilger[30] points out, in the one-step mechanism quenching occurs due to leakage of fuel and the corresponding temperature decrease on the rich side, while experiments and numerical calculations of counterflow methane flames show that leakage of oxygen on the lean side is the cause for quenching. In a 1983 GAMM-workshop on the numerical calculation of the methane-air stagnation point flame measured by Tsuji and Yamaoka[31] five different groups determined the flame structure of this flame using elementary kinetics with encouraging agreement[12]. Later on, Miller et al.[32] extended the calculation to more highly stretched flames to determine the extinction condition. The same numerical code was employed in ref. 33 using a reduced four-step mechanism for methane flames

I $CH_4 + 2 H + H_2O = CO + 4 H_2$
II $CO + H_2O = CO_2 + H_2$
III $2 H + M = H_2 + M$
IV $O_2 + 3 H_2 = 2 H + 2 H_2O$
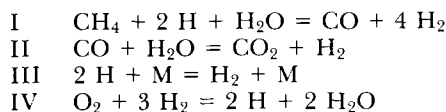
This mechanism was derived using steady state assumptions for the intermediates OH, O, HO_2, CH_3, CH_2O and CHO and partial equilibrium of the reactions $H_2 + OH = H + H_2O$ and OH $+ OH = O + H_2O$ in the same way as in ref. 16. The rates are those of the remaining elementary reactions of the C_1-chain, where the most important steps governing reactions I–IV are

I $CH_4 + H \rightarrow CH_3 + H_2$
II $CO + OH \rightleftarrows CO_2 + H$
III $H + O_2 + M \rightarrow HO_2 + M$
IV $H + O_2 \rightleftarrows OH + O$

Calculations of the diffusion flame structure for two velocity gradients across the flame, $a = 100$/sec and $a = 400$/sec corresponding to $\chi_{st} = 4$/sec and $\chi_{st} = 16$/sec, respectively, are shown in Figs. 2 and 3. The case $a = 400$/sec is very close to extinction. The maximum temperature drops from 2000 K for $a = 100$/sec to 1800 K for $a = 400$/sec while the leakage of oxygen increases by a factor of approximately 2.5. There is no leakage of fuel through the reaction zone. This may be understood by an asymptotic analysis[34] which leads to the flamelet structure shown in Fig. 4. On the lean side of stoichiometry there is a relatively broad layer of thickness $\epsilon < 1$, where ϵ is related to the Damköhler number (assumed to be large) of
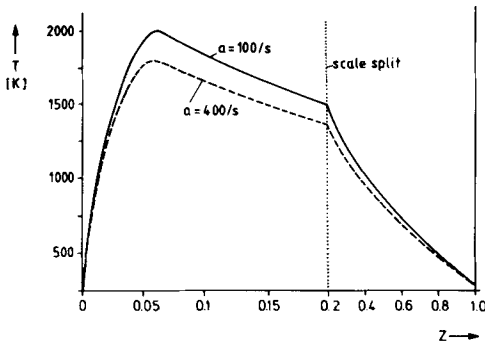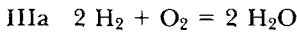
FIG. 2. Temperature as a function of the mixture fraction for a stagnation point diffusion flame. At the velocity gradient $a = 400$/sec the flame is close to extinction.

the chain breaking step H + O_2 + M→HO_2 + M. The H-radical is in steady state in this layer which leads to the global reaction

IIIa $2 H_2 + O_2 = 2 H_2O$

as a combination of reactions III and IV. The ε-layer is the broadest layer within the reacting part of the flame structure and therefore determines its overall thickness. Between this layer and the inert layer of order $O(1)$ on the fuel rich side, there is a thin fuel consumption layer of order $O(\delta)$, where δ is small and proportional to the ratio of the rates of the reactions H + O_2→OH + O and CH_4 + H→CH_3 + H_2. The radicals presented by the H-radical (to which O and OH are related by partial equilibrium assumptions) are in steady state except for a thin radical consumption layer embedded within the fuel consumption layer. The asymptotic flame structure is very similar to that of a premixed stoichiometric methane-air flame discussed in
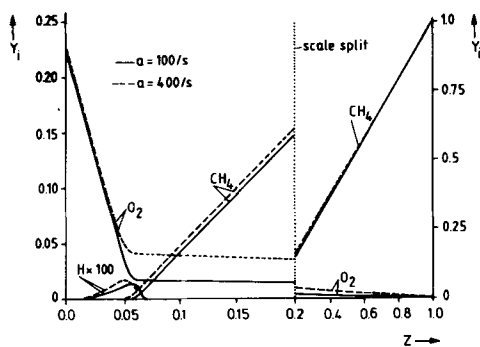

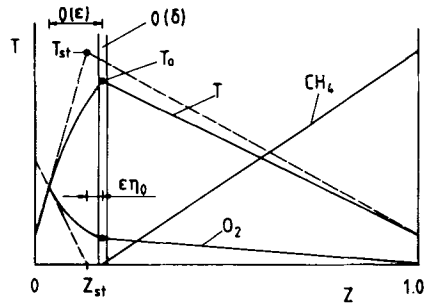FIG. 3. Some species mass fraction profiles corresponding to Fig. 2.

FIG. 4. Asymptotic structure of a methane-air diffusion flamelet.

section 3.2. An important difference is the diffusion of oxygen from the lean side and its leakage through the inner flame structure. On the rich side of the fuel consumption layer all radicals are depleted and the rich part of the flame structure therefore remains chemically inert. With an increasing velocity gradient the residence time is reduced, such that the reaction IV consumes less oxygen leading to a larger leakage. This in turn reduces the temperature due to coupling relations and decreases the highly temperature dependent reaction rate IV even further until, finally, the flamelet will extinguish.

In Fig. 5 the S-shaped curve for steady state diffusion flames is shown schematically. Here, the maximum temperature is plotted over the Damköhler number (for one-step kinetics) or over the inverse of χ_{st}, if the kinetics (elementary or global) are fixed. Burning of the flamelet corresponds to the upper branch of the curve. If χ_{st} is increased the curve is traversed to the left until χ_q is reached, beyond
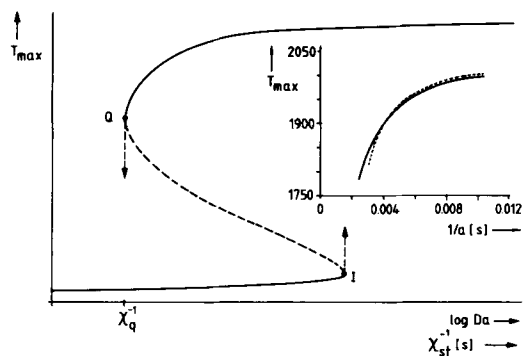

FIG. 5. The S-shaped curve for diffusion flames. The points Q and I correspond to quenching and ignition, respectively. Inserted are numerical results of the upper branch, using an elementary mechanism[32] - - - -, and a reduced four-step mechanism[33] ————.

which only the lower, extinguished steady state exists. The transition from the point Q to the lower state corresponds to an unsteady transition. Autoignition, which would correspond to an unsteady transition from the point I to the upper curve, is unlikely to occur in diffusion flames, since the required very large residence times (very small values of χ_{st}) never occur. Inserted into this picture are the numerical results from the calculations with an elementary mechanism[32] and with the reduced four-step mechanism[33]. The agreement is excellent except close to extinction, where the four-step mechanism predicts a larger velocity gradient of approximately $a \sim 400$/sec, while in ref. 32 approximately $a = 350$/sec is obtained.

One of the shortcommings of the steady state analysis of the flamelet structure is related to boundary conditions. It is assumed that the structure extends (as in a steady state counter-flow diffusion flame) from $x = -\infty$ on the rich side to $x = +\infty$ on the lean side which corresponds in the mixture fraction plane to applying the boundary conditions at $Z = 1$ and $Z = 0$. However, in particular close to the lift-off height of turbulent jet diffusion flames, fuel and air are partially premixed on both sides of the flamelets. Partial premixing of steady state diffusion flamelets has been considered in ref. 35 and experimental and numerical investigations of partially premixed counter-flow diffusion flames, showing excellent agreement, have been performed by Seshadri et al.[36] and Rogg et al.[37], respectively.

2.3 Two-variable statistical description of non-premixed turbulent combustion

The flamelet concept postulates that a turbulent diffusion flame consists of an ensemble of thin diffusion flamelets where reaction takes place. In ref. 28 five different states of a diffusion flamelet have been identified.

1. the steady unreacted initial mixture
2. the unsteady transition after ignition
3. the quasi-steady burning state
4. the unsteady transition after quenching
5. the unsteady transition after reignition

If one assumes that the unsteady transitions are not very frequent, only the two steady states 1 and 3 contribute to the overall statistical description of a turbulent diffusion flame. The unreacted state 1 is independent of χ_{st} but the burning state 3 depends on two parameters, Z and χ_{st}. In a turbulent flow field these parameters are statistically distributed. To predict non-equilibrium effects in turbulent diffusion flames, it is therefore necessary to predict the joint distribution function of Z and χ_{st}. In ref. 28 the properties of the joint probability density function of Z and χ_{st} have been discussed in detail and the relation to semi-empirical turbulence models of the k-ϵ-type have been pointed out. Liew et al.[38,39] have applied the flamelet concept based on the two variable description by assuming a two-delta function distribution of χ which leads to a splitting into a burning phase and a non-burning phase. They have calculated a library of stretched diffusion flamelets using elementary kinetics which were introduced into a numerical code that provides the overall turbulence properties of jet diffusion flames. This approach was recently extended using partially premixed diffusion flamelets by Rogg et al.[37].

Local quenching effects which lead to a disruption of the flame surface may have important consequences for turbulent diffusion flame stability. Starner and Bilger[40] have measured the electrical conductivity between the nozzle and the main flame brush in a specially designed piloted diffusion flame. They found intermittency in the electrical conductivity which points towards an interruption of the reacting (and therefore electrically conducting) flame surface and therefore towards local flame quenching. Likewise, Dibble et al.[41], using C_2-fluorescence as well as Rayleigh scattering, observed increasing local flamelet extinction in a turbulent methane jet diffusion flame as they increased the jet exit velocity.

In turbulent jet flames the mean scalar dissipation rate decreases with distance from the nozzle. Therefore, if a flame is burning far downstream, the probability of quenching of a flamelet increases with decreasing distance from the nozzle. But also there may be flamelets which were not reached by an ignition source and therefore stay unignited. Even within the turbulent flame brush there may be burnable yet unignited clusters of flamelets that are not connected to burning flamelets. A theory that is able to account for such a situation is percolation theory[28]. Percolation theory (cf. for instance Kirkpatrick[42]) describes the conduction in randomly distributed networks. For example, if holes are punched randomly into carbon paper[43], there will be a threshold, beyond which the probability that an electric current can pass from one side of the paper to the other decreases to zero. There is an analogy to lifted flames, where local quenching of diffusion flamelets corresponds to the holes in the carbon paper and the lift-off height to the percolation threshold[28]. In a first approximation, assuming zero variance of the probability distribution of χ_{st} and statistical

independence between Z and χ_{st}, the lift-off height should correspond to the downstream location where the mean scalar dissipation rate is equal to the laminar quenching value χ_q[44,45]. This prediction provides a basis for a verification of the flamelet concept. In ref. 46 measurements of stabilization heights in round methane-air jet flames diluted with nitrogen were performed. The stoichiometric mixture fraction Z_{st} was kept constant by also diluting the fuel. The residence times d/u_0 for each dilution, where d is the nozzle diameter and u_0 the exit velocity, were scaled with the corresponding value of χ_q obtained from an evaluation of the laminar counterflow flame results of Ishizuka and Tsuji[47]. Fig. 6 shows χ_q for the different dilutions, multiplied with the residence time d/u_0, plotted over the lift-off height H, divided by d. It is seen that this scaling of turbulent flame data with the laminar flamelet quenching parameter reduces the lift-off data to a single curve. The prediction is based on a k-ϵ-type turbulence model[45] using statistical independence of Z and χ_{st}.

In summary, the flamelet concept has proven to be useful for non-premixed combustion because it is a straight-forward extension of the local equilibrium model and because a two-variable statistical formulation, which resulted from the flame-attached coordinate transformation, appears to be a reasonable approximation. However, the importance of unsteady effects, not only for the prediction of scalars, needs to be explored further. For instance, a recent analysis[48] indicates that quenching events, which occur on a fast time scale, induce velocity changes which are of the same order of magni-

tude as the velocity fluctuations in a turbulent flame at blow-off. This would increase the turbulent kinetic energy and dissipation levels of the flow and mixing field and therefore should lead to a better agreement between prediction and data in Fig. 6. It also points towards more of a mutual interaction between combustion and turbulence. Nevertheless, the flamelet concept for non-premixed combustion, as it incorporates non-equilibrium effects, appears to be a promising tool for the investigation of important questions like flame stability, but also of NO_x-and soot-formation, which are yet to be explored.

3. The flamelet concept for premixed combustion

In premixed combustion the flamelets are not attached to a surface imposed by the mixing field as in non-premixed combustion, but they propagate normal to themselves into the unburnt mixture. Their location therefore depends on the flow field itself—rather than on the mixing field—and is determined by the interaction of the flame with the entire range of length and time scales of the oncoming flow. The fact that the flame is propagating leads to a characteristic velocity scale—the flame speed—and a characteristics length scale—the flame thickness. These scales have to be compared with characteristic scales of the flow field which defines different regimes of premixed turbulent combustion to be discussed below. The question of flamelet quenching which was quite important in non-premixed combustion, is now to be answered differently for the different regimes. In principle, premixed flamelets are not expected to extinguish as easily as diffusion flamelets, as they are embedded between the cold unburnt and the hot burnt gas rather than between two cold mixtures. They therefore loose heat only to one side and can receive heat and some chemically active radicals from the burnt gas side. Nevertheless, volumetric heat loss, for instance by radiation, or differential diffusion combined with flame stretch, but also diffusion of radicals out of the reaction zone and chemical effects close to the flammability limits[49] will enhance local extinction of flamelets. Compared to diffusion flamelets, premixed flamelets may be expected to recover much more easily from such extinction events. All these considerations suggest that the unsteady response of premixed flamelets leading to a much more vigorous dynamical interaction with the flow field must be considered.

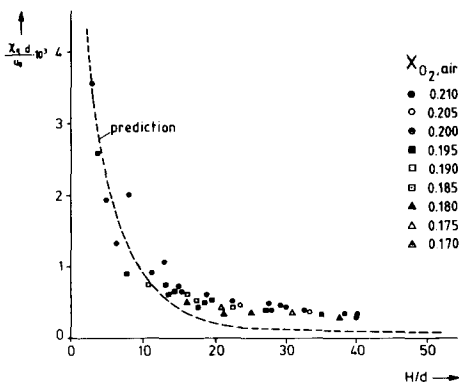A recent review on laminar flamelet mod-

FIG. 6. The laminar quenching value χ_q, nondimensionalized with the turbulent flame residence time d/u_0 plotted over the nondimensional lift-off height H/d for different mole fractions X_{O_2} of oxygen in air.

elling that emphasises the common features of the approach for both, premixed and diffusion flamelets, was given by Bray[50]. A forthcoming review by Pope[51] on premixed flames in general focusses on the pdf approach and modelling aspects.

3.1 Flamelet regimes and the Gibson scale

Several authors (Bray[52], Williams[8], Borghi[53]) have supplied phase diagrams to illustrate different regimes in premixed turbulent combustion as a function of dimensionless quantities. Those are the turbulent Reynolds number

$$Re = \frac{v'\ell_t}{\nu}, \quad v' = \sqrt{\frac{\overline{v_k'^2}}{3}}, \tag{13}$$

the turbulent Damköhler number

$$Da = \frac{t_t}{t_F} = \frac{v_F \ell_t}{v' \ell_F} \tag{14}$$

and the turbulent Karlovitz number

$$Ka = \frac{\gamma \ell_F}{v_F} = \frac{t_F}{t_k}, \quad \gamma = \frac{1}{t_k} = \sqrt{\frac{\epsilon}{\nu}}. \tag{15}$$

In eqs (13)–(15) v' is the turbulence intensity, ℓ_t and $t_t = \ell_t/v'$ are the macro length and time scales and ν is the laminar viscosity. The laminar flame speed v_F, the laminar flame thickness ℓ_F and the flame time t_F are related to each other by

$$v_F \ell_F = \nu, \quad t_F = \ell_F/v_F , \tag{16}$$

if we assume a Prandtl number of unity, which is accurate enough for the order of magnitude arguments to follow (alternatively, eq. (16) may be viewed as definition for ℓ_F.) Furthermore, γ is the inverse of the Kolmogorov time $t_k = \ell_k/v_k$ and describes the straining by the smallest eddies of the Kolmogorov size $\ell_k = (\nu^3/\epsilon)^{1/4}$ which have a circumferential velocity $v_k = (\nu\epsilon)^{1/4}$. Here ϵ is the dissipation of the turbulent kinetic energy in the unburnt gas. With v' and ϵ prescribed, the macro length scale of the energy containing large eddies may be defined by

$$\ell_t = \frac{v'^3}{\epsilon}. \tag{17}$$

These definitions can be used to derive the following relations between the ratios v'/v_F and ℓ_t/ℓ_F in terms of the three non-dimensional numbers Re, Da and Ka as

$$\frac{v'}{v_F} = Re\left(\frac{\ell_t}{\ell_F}\right)^{-1}, \quad \frac{v'}{v_F} = Da^{-1}\frac{\ell_t}{\ell_F},$$
$$\frac{v'}{v_F} = Ka^{2/3}\left(\frac{\ell_t}{\ell_F}\right)^{1/3} \tag{18}$$

as well as the relation

$$Re = Da^2 Ka^2. \tag{19}$$

In the following we will adopt a modified version of Borghi's[53] phase diagram and plot the logarithm of v'/v_F over the logarithm of ℓ_t/ℓ_F in Fig. 7. In this diagram the lines $Re = 1$, $Da = 1$ and $Ka = 1$ represent boundaries between the different regimes of premixed turbulent combustion. Another boundary of interest is the line $v'/v_F = 1$ which separates wrinkled from corrugated flamelets.

The regimes of laminar flames ($Re < 1$) and the well-stirred reactor ($Da < 1$) are not of interest in the present context. Among the remaining three regimes the wrinkled flames and the corrugated flames belong to the flamelet regime which is characterized by the inequalities $Re > 1$ (turbulence), $Da > 1$ (fast chemistry) and $Ka < 1$ (sufficiently weak flame stretch). The boundary to the distributed reaction zones regime given by $Ka = 1$ may be expressed in view of

$$Ka = \frac{t_F}{t_k} = \frac{\ell_F^2}{\ell_k^2} = \frac{v_k^2}{v_F^2} \tag{20}$$

as the condition where the flame thickness is equal to the Kolmogorov scale. This is the Klimov-Williams criterion[54,55]. The distributed reaction zones regime is characterized by $Re > 1$, $Da > 1$ and $Ka > 1$, the last inequality
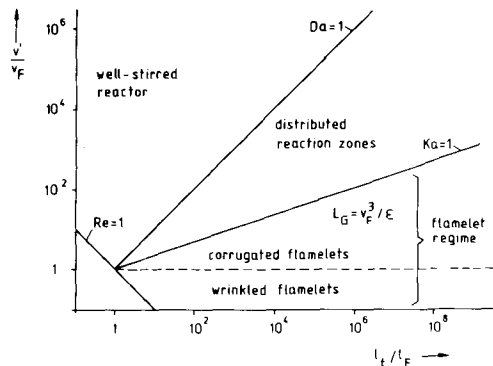
FIG. 7. Phase diagram showing different regimes in premixed turbulent combustion.

indicating that flame stretch is strong and that the smallest eddies can enter into the flame structure since $\ell_k < \ell_F$, thereby broadening the flame structure. These eddies produce the largest straining rates and may lead to local extinction of some inner reaction zone, but nothing definite is known about this interaction at present.

The flamelet regime is subdivided into the regimes of wrinkled flamelets and corrugated flamelets. This boundary is viewed by Williams[8] as the one between single and multiple flame sheets. Clearly, if $v' < v_F$ and v' is interpreted as the circumferential velocity of the large eddies, even those eddies cannot enough convolute the flame front to form multiply connected reaction sheets. In the regime of wrinkled flamelets, asymptotic methods using large activation energy have been a very powerful tool to describe the interaction between weak turbulence and the flame front. An excellent recent review on theoretical as well as on experimental verifications by the group at Marseille (cf. Sabathier et al.[56], Boyer et al.[57], Searby et al.[58,59]) is due to Clavin[60]. Notably the theoretical work by Clavin and Williams[5,61], Clavin and Joulin[62], Clavin and Garcia[63], Pelcé and Clavin[64], Sivashinsky[65-68] (cf. also the review paper by Sivashinsky[69]), Buckmaster[70-73], Buckmaster and Mikolaitis[74], Matalon and Matkowsky[75], Margolis and Matkowsky[76] has contributed to our understanding of flame instability and of the response of a thin flame to stretch imposed by a non-uniform flow field. Flame stretch, which was introduced by Karlovitz et al.[77], is the local fractional increase of flame -surface area (cf. Buckmaster[73], Matalon[78], Chung and Law[79]). In a steady flow field positive flame stretch is an addition of the effect of straining by flow divergence and of positive flame curvature (cf. Fig. 8). For a one-step reaction an essential additional factor is differential diffusion of heat and the deficient reactant characterized by its Lewis number

$$Le = \frac{\lambda}{\rho c_p D} \qquad (21)$$

which is enhanced by flame stretch and induces a temperature change at the thin reaction layer. Due to the large activation energy of a single global reaction, that was assumed in all the theoretical work in refs. 5,61–76, the flame speed is very sensitive to temperature changes. Positive stretch increases the enthalpy and thereby the temperature in the thin reaction layer if $Le < 1$ and decreases it if $Le > 1$. The flamelet responds therefore by an acceleration if flame stretch is positive and $Le < 1$ or negative flame stretch and $Le > 1$, and by a
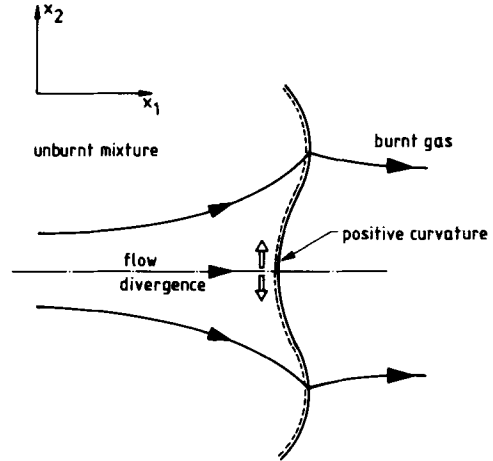

FIG. 8. Schematic illustration of flow divergence and curvature leading to flame stretch in premixed combustion.

deceleration if flame stretch is negative and $Le < 1$ or positive flame strech and $Le > 1$. It follows that cellular patterns will form for $Le < 1$ because an initial perturbation of the flame front is enhanced, while the $Le > 1$ case is stabilizing. A numerical simulation of the response of premixed flames in random turbulent flow fields has been performed recently[80] for the two cases $Le = 0.5$ and $Le = 2.0$. These flames had a (v'/v_F)-ratio of about one and a (ℓ_t/ℓ_F)-ratio much larger than one. Excess enthalpy contours (the excess enthalpy is defined as the enthalpy minus that of a plane undisturbed flame) are shown for $Le = 0.5$ and $Le = 2.0$ in Fig. 9a and 9b, respectively. The flames propagate from the right to the left in these
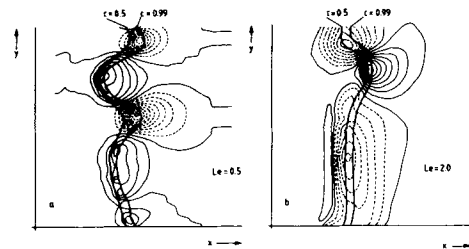

FIG. 9. Excess enthalpy contours of premixed flames with non-unity Lewis numbers in random turbulent flow fields[80]. Contours of positive and zero excess enthalpies are denoted by continuous lines, while negative excess enthalpy contours have dotted lines. Fig. 9a: $Le = 0.5$, showing manifestation of cellular instability, Fig. 9b: $Le = 2$, showing a stabilizing effect.

pictures. For $Le = 0.5$ a cellular structure of the flame front (represented by the lines $c = 0.5$ and $c = 0.99$, where c is the progress variable) is observed in Fig. 9a with hot spots (positive excess enthalpy) at the leading parts of the front and cold spots (negative excess enthalpy) at the troughs. On the contrary, in the $Le = 2.0$ case shown in Fig. 9b, a hot spot develops in the upper part of the flame that has been left behind while the more advanced parts of the flame front show negative excess enthalpies. The hot spot will cause the flame front to accelerate locally smoothing out the perturbations induced by the random turbulent flow field. A total number of 67 numerical realizations has been analysed. Among other statistical data a correlation between excess enthalpy and normal strain has been found. This is a measure of the dynamic response of premixed flamelets and makes a quasi-static description, which was successful for diffusion flamelets, quite suspect.

The regime of corrugated flamelets is much more difficult to analyse analytically or numerically. In view of eq. (20) we have with $Ka < 1$ within this regime

$$v' \geq v_F \geq v_k. \qquad (22)$$

Since the velocity of the large eddies is larger than the flame speed, these eddies will push the flame front around, causing a substantial convolution. On the other hand the smallest eddies, having a circumferential velocity less than the flame speed, will not wrinkle the flame front. We may construct a discrete sequence of eddies within the inertial range by defining

$$\ell_n = \frac{\ell_t}{a^n}, \quad \ell_n \geq \ell_k, \quad n = 0, 1, 2, \ldots \qquad (23)$$

where $a > 1$ is an arbitrary number. Then, energy cascade arguments require that ϵ is independent of n and dimensional scaling laws lead to a circumferential velocity v_n as

$$v_n^3 = \epsilon \ell_n \qquad (24)$$

indicating that the velocity decreases as the size of the eddy decreases.

Now, as illustrated in Fig. 10, we want to determine the size of the eddy which interacts locally with the flame front by setting the circumferential velocity v_n equal to the flame speed v_F. I want to call this characteristic size
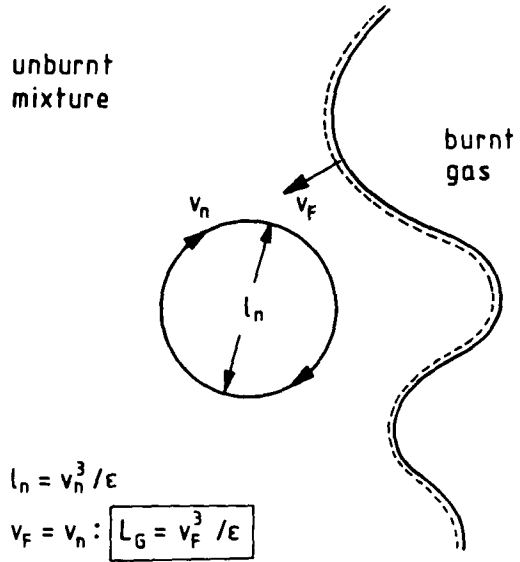
$$L_G = \frac{v_F^3}{\epsilon}, \qquad (25)$$

$$l_n = v_n^3 / \epsilon$$

$$v_F = v_n : \boxed{L_G = v_F^3 / \epsilon}$$

FIG. 10. The interaction of eddies ℓ_n from the inertial range of turbulence with a flame front. An eddy of Gibson scale L_G has a circumferential velocity equal to the flame velocity.

the Gibson scale[*]. It is the size of the burnt pockets that move into the unburnt mixture, try to grow there due to the advancement of the flame front normal to itself, but are reduced in size again by newly arriving eddies of size L_G. Therefore, there is an equilibrium mechanism for the formation of burnt pockets, while unburnt pockets that penetrate into the burnt gas will be consumed by the flame advancement. A more detailed derivation is given in ref. 81, where also some preliminary experimental data are presented. In particular, it is worth noting that L_G increases with v_F if the turbulence properties are kept constant. At sufficiently low turbulence levels, the mean thickness of a turbulent flame should be influenced by this mechanism and therefore also increase with v_F. This is observed in the V-shaped flame by Namazian et al.[82], where the mean flame thickness increases by a factor between 2 and 3, as the equivalence ratio is changed from $\phi = 0.6$ to $\phi = 0.8$, thereby increasing v_F. On the contrary, the size of

cellular wrinkles due to the instability mechanism described above decreases with v_F, since it is proportional to ℓ_F which decreases with v_F according to eq. (16). Using eq. (17), one may also write eq. (25) in the form

$$\frac{L_G}{\ell_t} = \left(\frac{v_F}{v'}\right)^3. \tag{26}$$

An illustration of the kinematics of the interaction between a premixed flame and a turbulent flow field may be found in Fig. 9 of the paper by Ashurst and Barr[83]. In this numerical study the characteristic macro length scale ℓ_t was kept constant while the turbulence intensity was increased, showing corrugations of smaller and smaller size. A similar effect is observed in the 2-D visualisations of the flame front in I.C. engines by Baritaud and Green[84] and zur Loye and Bracco[85] with increasing engine speed. Here it may be argued that the macro length scale is determined by the geometrical dimensions of the combustion chamber and that the turbulence intensity increases linearly with engine speed. Since eddies smaller than L_G (but larger than ℓ_k) will not wrinkle the flame front, L_G has the character of a lower cut-off scale. This property of the L_G-scale will be used in the context of fractal dimensions in section 3.4.

3.2 The response and inner structure of stretched steady state premixed flamelets

As in non-premixed combustion it is useful in premixed combustion to introduce a coordinate system attached to the flame front and—with the assumption that the flamelet is thin—analyse the one-dimensional flamelet structure and its response to flame stretch. For weak stretch in steady flow fields it has been shown by Sivashinsky[65] and Buckmaster and Ludford (cf. ref. 7, p. 146) that flow divergence and curvature have an equivalent influence. Therefore, as a first step in analysing the influence of chemistry and heat loss it is illuminating to calculate the response of a plane flame in a diverging flow field. This has been done numerically by Libby et al.[86-89] in a series of papers for a one-step mechanism with a large activation energy and weak to strong strain. Lewis number effects[88,89] and heat loss to the burnt gas[87] as well as density effects are considered. It is concluded that a Lewis number larger than one and heat loss promotes flame extinction, but that it is retarded by density

changes. A numerical analyses of the problem in ref. 86, that resolves the thin reaction zone, has been performed by Darabiha et al.[90]. Experimental work on stretched twin flames[89] was performed by Sato and Tsuji[91], Sato[92], Sohrab et al.[93] and Chung et al.[94]. Again asymptotically, for weak strain the effect of intermediates in a two-step mechanism was found to retard extinction[95] (cf. also refs. 96–97), if the activation energy of the first reaction is large. The interaction of weak stretch and heat loss with chemical extinction effects at the lean flammability limit (due to the modelled competition of the reactions $H + O_2 \rightarrow OH + O$ and $H + O_2 + M \rightarrow HO_2 + M$) was analysed in ref. 49. These papers, although they use model reactions, indicate that the presence of intermediates may influence the response of premixed flames considerably.

Stretched lean ($\phi = 0.6$) and rich ($\phi = 1.4$) hydrogen-air flames with elementary kinetics have been analysed numerically in ref. 15. Due to the large diffusivity of hydrogen, the Lewis number is 0.3133 in the lean case and due to the large thermal diffusivity it is 3.018 in the rich case. Therefore, in both cases the Lewis number differs considerably from one. The results show that in this case the Lewis number effect is dominating over details of the chemical kinetics and that Sivashinsky's[65] analysis for weak stretch is a good approximation for the flame response. In particular, extinction is found for positive stretch in the rich hydrogen flame. The Karlovitz number at extinction was found to be as small as 0.029 in agreement with prediction. Recently, Rogg[98] has calculated stretched methane flames on the basis of the reduced four-step mechanism derived in ref. 16 which was discussed in section 2.2. The structure of the corresponding unstretched flame is analysed asymptotically in ref. 99 and is presented schematically in Fig. 11a. Steady state of H has been assumed here which reduces the four-step mechanism to a three-step mechanism with reaction I replaced by

Ia $CH_4 + O_2 = CO + H_2 + H_2O$
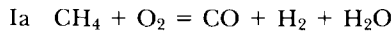
and reaction III by IIIa (cf. section 2.2). In terms a coordinate nondimensionalized with ℓ_F the flame structure consists of a chemically inert preheat zone of thickness $O(1)$, a thin fuel consumption layer of thickness δ, where CH_4 is consumed and H_2 and CO are formed due to reaction Ia, and a downstream CO/H_2-oxidation layer of thickness ϵ governed by the rate of the reaction $H + O_2 + M \rightarrow HO_2 + M$. At the leading edge of the oxidation
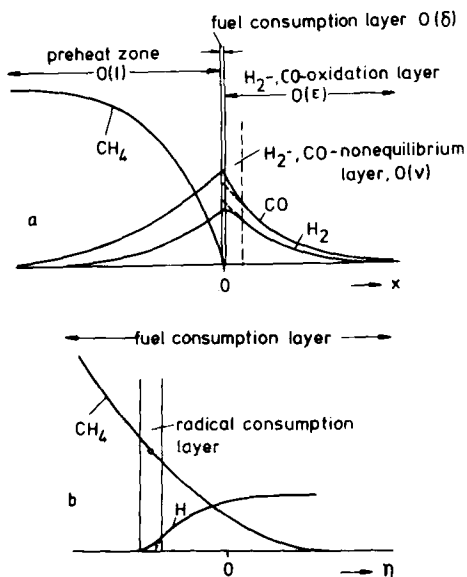
FIG. 11. Asymptotic inner structure of premixed stoichiometric methane-air flamelets. Fig. 11a shows three layers embedded within each other and Fig. 11b a blow-up of the fuel consumption into which a radical consumption layer is embedded.

FIG. 12. Maximum H and H_2 mass fraction, flame position η and mass flow rate as function of the velocity gradient in a counterflow premixed stoichiometric methane flame from ref. 98. The flame position is defined by the maximum of the methane consumption rate and η defined as in ref. 86.

layer there is a nonequilibrium layer of reaction II with thickness ν which tends to equilibrium downstream. The ordering of the relative width of the layers is $\delta < \nu < \epsilon < 1$. No activation energy appears as an expansion parameter in the analysis, the crucial cut-off of the chemistry in the fuel consumption layer being essentially due to depletion of radicals by the fuel according to the reaction $CH_4 + H \rightarrow CH_3 + H_2$ in a thin radical consumption layer embedded within the fuel consumption layer as shown in Fig. 11b.

The numerical calculations by Rogg[98] were performed for stoichiometric methane flames in a counterflow of unburnt mixture and equilibrium burnt gas similar to the flow in ref. 86. As seen from Fig. 12, the flame is quenched by a velocity gradient $a = 2270/\text{sec}$, when the fuel consumption layer nearly reaches the stagnation point. Therefore, the flame velocity is nearly zero at quenching, which is different from the hydrogen flames analysed in ref. 15. The quenching mechanism here is not differential diffusion of heat and reactants, but enhanced diffusion of the hydrogen radical to both sides of the flame, to the unburnt mixture as well as to the burnt gas. When the inner flame structure reaches the stagnation point, the gradient of the H-profile towards the burnt
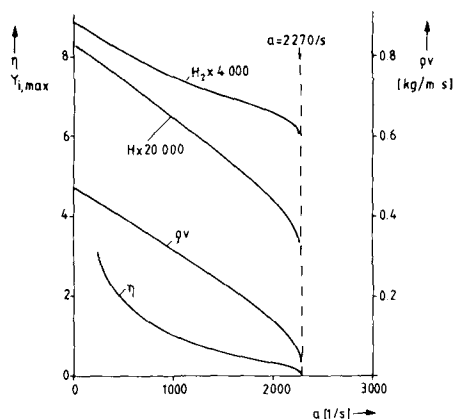
gas is drastically increased, such that production of H by chain-branching reactions can no longer balance the losses. In Fig. 12 it is seen that quenching occurs at a non-zero maximum value of Y_H and Y_{H_2} with a vertical tangent of these curves. The mechanism resembles that of diffusion flamelet quenching, where heat losses to both sides cannot be balanced by heat production and quenching occurs at a temperature well above ambient. Again, the Karlovitz number at quenching, defined as in ref. 15, is 0.15, thereby sufficiently less than one, such that quenching is possible in the flamelet regime.

Another interesting outcome from Rogg's analysis are the plots of the temperature and the mass fractions of H, CH_4, O_2 and H_2O, shown in Figs. 13 and 14, over that of CO_2. The mass fraction of CO_2 was chosen to present the progress variable c used in the BML-model. It has the advantage to be produced only by a single reaction in the downstream oxidation layer, while the temperature or any other species take part in several reactions. Figs. 13 and 14 show that the scalar structure is changed by flame stretch, while the BML-model assumes linear relations between all scalars, which would correspond to straight lines in these figures. A formulation similar to the two parameter statistical description of diffusion flamelets could be developed using the mass fraction of CO_2 and the strain rate (or an equivalent stretch parameter that includes the influence of curvature) as two parameters in analogy to Z and χ, respec-
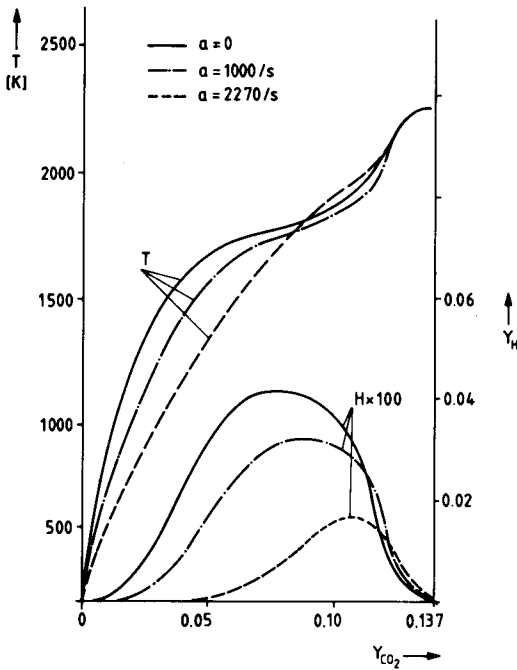
FIG. 13. Temperature and H mass fraction plotted over the mass fraction of CO_2 showing the scalar structure of stretched premixed flamelets (from ref. 98).
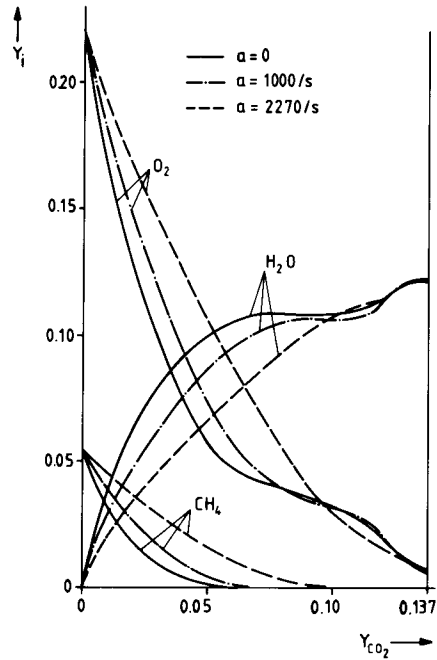

FIG. 14. Methane, oxygen and water vapour mass fractions plotted over the mass fraction of CO_2 for the stretched premixed flamelets from ref. 98.

tively. However, since Y_{CO_2} is not a conserved scalar like the mixture fraction, its moments or pdf cannot be calculated independently of the chemistry that occurs within the flamelets.

3.3 Statistical flamelet models in premixed turbulent combustion

The most prominent statistical description of premixed turbulent combustion in the flamelet regime is the Bray-Moss-Libby (BML) model which uses second order closure of moment equations. It has been developed in a series of papers[100-109] and progress has also been presented in the several reviews[52,110-112]. The model assumes $Le = 1$ and uses a presumed pdf for the progress variable c which may be viewed either as the normalized product mass fraction or as the normalized temperature, both varying between zero and one. By presuming a two-delta function pdf at $c = 0$ and c = 1, thereby introducing the concept of a thin flamelet embedded within the turbulent flow, the model is able to express Favre mean quantities such as the mean velocity $\bar{u}$, the scalar flux $\overline{u''c''}$ and higher moments as functions of conditional

moments at $c = 0$ and $c = 1$. The expression for the scalar flux in a normal flame is, for example,

$$\widetilde{u''c''} = \bar{c}(1 - \bar{c}) (\bar{u}_p - \bar{u}_r), \qquad (27)$$

$\bar{c}$ is the Favre mean progress variable and $\bar{u}_p$ and $\bar{u}_r$ are the conditional mean velocities of the reactants and the products in x-direction, respectively. The boundary conditions are $\bar{c} = 0$ at $x \to -\infty$ and $\bar{c} = 1$ at $x \to +\infty$. Since in a normal flame there is a self-induced mean pressure drop, the light products will accelerate relative to the heavier reactants such that $\bar{u}_p > \bar{u}_r$, in the major parts of the turbulent flame if the density difference is sufficiently large. It follows that $u''c'' > 0$ in contrast to the gradient flux approximation

$$\widetilde{u''c''} = - D_t \frac{\partial \bar{c}}{\partial x}, \qquad (28)$$

where D_t is a (positive) turbulent diffusivity and the mean progress variable gradient is positive in the flame.

Although the BML-model uses a certain number of assumptions, in particular about the chemistry, it provides an important physical insight and predicts a large number of interesting features in agreement with experiments,

such as scalar transport and turbulence production[113], and crossing frequency statistics[82,114-116]. A shortcoming of the model is its inability to predict the turbulent flame speed, which in turn is required as an input to the calculations performed in a phase plane with $\bar{c}$ as independent variable. The spatial structure of the turbulent flame could only be resolved, if in addition the mean reaction rate was known. It has been shown[103] that the mean reaction rate is proportional to the dissipation rate of the progress variable χ_c, or to the inverse of the mean crossing frequency t_m[106,107], but this does not close the problem. Since χ_c is influenced by both, the straining of the scalar field by the flow field and the scalar gradients generated by the flamelets, there is no convincing model available for this quantity. This situation is fundamentally different from that in non-premixed combustion, where the scalar dissipation of the conserved scalar Z, which is independent of chemistry, represents the characteristic diffusion time. As far as the modelling of the mean crossing frequency t_m is concerned, it seems evident that the time scale $T_G = L_G/v_F$, the turnover-time of the eddies of the Gibson scale, should enter as a lower cut-off time.

Another promising approach to premixed turbulent flamelet combustion is the solution of a pdf equation by Pope and Anand[21], Anand and Pope[117] (cf. also ref. 51) using a Monte-Carlo method. They consider two cases:

1. The classical pdf-equation formulation where molecular diffusion is modelled in the same way as for chemically inert turbulent flow, which they call the case of distributed combustion and
2. a flamelet formulation where the chemical source term is replaced by the sum of the source term and the diffusive term, both expressed as a function of the progress variable and determined from the solution of a plane laminar flame.

In their recent work[117] they have added the effect of density changes and find striking agreement with many predictions by the BML-model including the manifestation of counter-gradient diffusion. The pdf equation approach is more general than the BML-model because a number of terms, for instance the correlation between velocity fluctuations and the chemical source term $\overline{u''S}$ and the second and third conditional moments of the velocity need not to be modelled, but are calculated on the basis of the pdf equation. The authors also predict the turbulent flame speed and obtain a linear relation $u_T \sim u'$, where the constant of proportionality changes from 2.1 for constant density

flames to 1.5 for large density ratios[117]. However, quoting Pope[51]: "Pope and Anand's result that the turbulent flame speed scales with u' (specifically $u_T = 2.1 \, u'$) is a direct consequence of the assumption that the mixing rate is proportional to τ^{-1}" (the inverse of the turbulent macro time scale, Pe.) "independent of u_L/u'." This remark refers to the fact that the model contains, in addition to the consideration of diffusion in the flamelet structure, a standard mixing model which causes pure ($c = 0$) reactants to be mixed with material $c > 0$ at a rate proportional to τ^{-1}. It is not clear to what extend this modelling assumption, which accentuates the behaviour at the cold boundary, i.e. $c = 0$, predetermines the results.

3.4 Attempts to predict the turbulent flame speed

In spite of the acquired understanding of the structure of premixed turbulent flames, the central problem of practical interest, the prediction of the turbulent flame speed, remains unresolved. A large body of experiments has been provided by the Leeds group (cf. Abdel-Gayed, Bradley et al.[118-123]) using the double kernel method during explosions in a fan-stirred combustion bomb. These data cover a large range of v'/v_F-ratio, of turbulent Reynolds number and a large number of different fuels. Although the scatter of the data permits a variety of interpretations, a general feature of the data is the bending of the curves v_T/v_F plotted over v'/v_F, where v_T is the turbulent flame speed. This behaviour has been discussed in the context of spark ignition engines in detail by Abraham et al.[124] where further experimental work is referenced.

Among the theoretical work based on flamelet considerations there is in particular the study by Klimov[125] (cf. also Klimov[126]). Klimov considers the evolution of the turbulent flame surface, originally convoluted by the turbulence, during a time interval until opposite fronts merge due to flame propagation. He obtains

$$\frac{v_T}{v_F} = \left(\frac{v'}{v_F}\right)^n, \quad n = 0.7 \qquad (29)$$

and claims good agreement with data. A shortcoming of the analysis is that only a single length scale of the flame surface is considerd. Recently Kerstein[127] has developed a pair-exchange model based on the idea of random exchange of fluid elements in direction normal to the flame. He obtains an exponent of $n = 0.5$ in the relation $v_T \sim (v')^n$ for very large values of the turbulent Reynolds numbers and $n > 0.5$

for not so large values. This interesting model considers the entire range of length scales, ranging from the Kolmogorov scale to the integral scale, to be present in the flame surface. However, in view of the discussion in section 3.1 we would expect that scales larger than the Kolmogorov scale but smaller than the Gibson scale L_G will not appear in the flame surface because the circumferential velocity of these eddies is too small to interact with the flame motion.

A different approach to predict the turbulent flame speed has recently been proposed by Gouldin[128]. He applies the concept of statistical geometry known as fractals advocated by Mandelbrot[129-131] to the geometry of the flame surface. The derivation starts from Damköhler's[132] observation that the ratio of the turbulent to the laminar flame speed should be proportional to the ratio of the instantaneous flame surface area A_t of the turbulent flame to the cross-sectional area A of the flow

$$\frac{v_T}{v_F} = \frac{A_t}{A}. \tag{30}$$

Now, according to the concepts of statistical geometry, homogeneous turbulence is not space-filling but has a fractal dimension between 2 and 3. This concept is related to the intermittent nature of turbulence (cf. Frisch et al.[133]). A recent evaluation of measurements in turbulent clouds by Hentschel and Procaccia[134] suggests a fractal dimension of 2.35. A basic feature of fractal dimension is the dependence of the geometry on the length scale ℓ with which it is measured, for a fractal surface area

$$A_\ell \sim \ell^{2-D} \tag{31}$$

where D is the fractal dimension. This indicates that the surface area in a turbulent flow increases like $A_\ell \sim \ell^{-0.35}$, if $D = 2.35$, as the length scale decreases, because smaller measuring scales can better resolve the finer structure of the surface. Gouldin[128] argues that as in non-reacting turbulence the true surface area A_t should be the one measured with $\ell = \ell_k$, the Kolmogorov scale, while the cross-sectional area A should be the one measured with the macro length scale ℓ_t.

Again, based on the argument about the Gibson scale as lower cut-off for the length scales that appear in a flame surface, we want to replace ℓ_k by L_G and write eq.(30) as

$$\frac{v_T}{v_F} = \left(\frac{L_G}{\ell_t}\right)^{2-D} = \left(\frac{v'}{v_F}\right)^{3(D-2)} \tag{32}$$

where eq. (26) was used. As far as the fractal dimension of the flame front is concerned, it is expected that D approaches the value 2.35 for very large values of v'/v_F where the motion of the front normal to itself is negligible compared to the turbulent motion. For not so large values of v'/v_F, however, the flame motion would smooth out the surface, thereby decreasing D. Cheng[135] and Tromans recently have evaluated some data from ref. 84 and find a fractal dimension of $D = 2.167$, whereas we find a value of $D = 2.20$ for the data ref. 84 and $D = 2.13$ for our own V-shaped flame data[81]. This is shown in Fig. 15. Thus, the combination of totally independent findings such as Gibson scale and the fractal dimension of a turbulent flame front yields exponents in eq. (29) between $n = 1.05$ for $D = 2.35$ and $n = 0.4$ for $D = 2.13$ which cover the entire range of turbulent flame speed measurements. This does not solve the turbulent flame speed problem, but it lends additional support for the Gibson scale as the lower cut-off scale in a turbulent flame front. More experimental work such as refs. 84–85 and an evaluation in terms of fractal dimension and the inner cut-off scale L_G would be highly desirable.

4. Summary

The inner structure of premixed and diffusion flamelets in a turbulent flow consists of several layers embedded within each other. A common feature of both is the response of this inner structure to flame stretch and the possibility of local quenching. However, the quench-
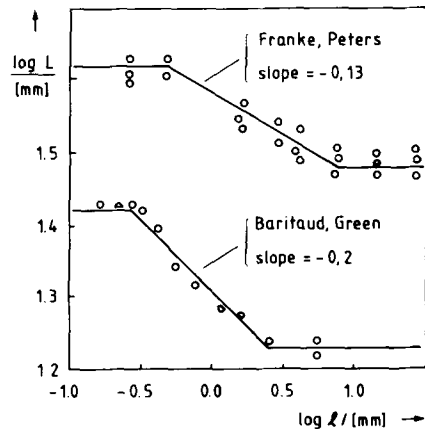

FIG. 15. Evaluation of fractal dimension D of flame contours from ref. 81 and 84. The slope corresponds to $2 - D$.

ing mechanism is different and the flame stretch required to achieve quenching of premixed flamelets is much larger than for diffusion flamelets. Furthermore, a genuine property of premixed flamelets not shared by diffusion flamelets is their ability to propagate and to interact with eddies of a specific scale, the Gibson scale. This interaction as well as the manifestation of *stabilizing* or *destabilizing* Lewis number effects in turbulent flames make their response much more dynamic than that of diffusion flamelets. For diffusion flamelets, a two-variable quasi-static statistical formulation appears to be a plausible approximation. A similar procedure bears some potential for premixed flames as far as local quenching is concerned, but the prediction of the most important statistical quantity, i.e. the turbulent flame speed, remains unsolved. It seems evident that the properties of the turbulent flow cannot be represented by a single time or length scale, but that the entire spectrum from the largest energy containing eddies to the lower cut-off scale will manifest itself for instance, in a statistical description of the turbulent flame surface.

REFERENCES

1. PRANDTL, L.: Verhandlg. III Intern. Math. Kongr. Heidelberg, 484–491 (1904).
2. ZEL'DOVICH, Y.B., FRANK-KAMENETSKII, D.A.: Zhur. Fiz. Khim. *12*, 100 (1938).
3. LIÑÁN, A.: On the internal structure of laminar diffusion flames, Technical note, Instituto nacional de tecnica aeronautica, Esteban Terradas, Madrid (1961).
4. BUSH, W.B., FENDELL, F.E.: Combust. Sci. Technol. *1*, 421 (1970).
5. CLAVIN, P., WILLIAMS, F.A.: J. Fluid Mech. *90*, 589 (1979).
6. PETERS, N.: Combust. Sci. Technol. *30*, 1 (1983).
7. BUCKMASTER, J.D., LUDFORD, G.S.S.: Theory of laminar flames, Cambridge University Press, 1982.
8. WILLIAMS, F.A.: Combustion Theory, 2nd Edition, The Benjamin/Cummings Publishing Company, Menlo Park, 1985.
9. WARNATZ, J.: Eighteenth Symposium (International) on Combustion, p. 369, The Combustion Institute, 1981.
10. WARNATZ, J.: Nineteenth Symposium (International) on Combustion, p. 197, The Combustion Institute, 1982.
11. WESTBROOK, C.K., DRYER, F.L.: Progr. Energy Combust. Sci. *10*, 1 (1984).
12. DIXON-LEWIS, G., DAVID, T., GASKELL, P.H., FUKUTANI, S., JINNO, H., MILLER, J.A., KEE, R.J., SMOOKE, M.D., PETERS, N., EFFELSBERG, E., WARNATZ, J., BEHRENDT, F.: Twentieth Symposium (International) on Combustion, p. 1893, The Combustion Institute, 1984.
13. PETERS, N., WARNATZ, J. (Eds.): Numerical Methods in Laminar Flame Propagation, Vieweg, Braunschweig, 1982.
14. DIXON-LEWIS, G.: *Combustion Chemistry* (W.C. Gardiner, Ed.), p. 21, Springer, 1984.
15. WARNATZ, J., PETERS, N.: Progress in Astronautics and Aeronautics *95*, 61 (1984).
16. PETERS, N.: Lecture Notes in Physics *241*, 90 (1985).
17. PACZKO, G., LEFDAL, P.M., PETERS, N.: Reduced reaction schemes for methane, methanol and propane flames, This Symposium (1986).
18. FENDELL, F.E.: J. Fluid Mech. *56*, 81 (1972).
19. LIÑÁN, A.: Acta Astronautica *1*, 1007 (1974).
20. POPE, S.B.: Progr. Energy Combust. Sci. *11*, 119 (1985).
21. POPE, S.B., ANAND, M.S.: Twentieth Symposium (International) on Combustion, p. 403, The Combustion Institute, 1984.
22. EFFELSBERG, E., PETERS, N.: Combust. Flame *50*, 351 (1983).
23. PITZ, R.W., DRAKE, M.C.: AIAA-paper 84-0197 (1984).
24. DRAKE, M.C., PITZ, R.W., SHYY, W.: J. Fluid Mech. *171*, 27 (1986).
25. CHEN, J.Y.: Combust. Flame *69*, 1(1987).
26. PETERS, N., HOCKS, W., MOHIUDDIN, G.: J. Fluid Mech. *110*, 411 (1981).
27. EICKHOFF, H.: Progr. Energy Combust. Sci. *8*, 159 (1982).
28. PETERS, N.: Progr. Energy Combust. Sci. *10*, 319 (1984).
29. PETERS, N., WILLIAMS, F.A.: Progress in Astronautics and Aeronautics *95*, 37 (1984).
30. BILGER, R.W.: Simplified Kinetics for Diffusion Flames of Methane in Air, submitted to Combustion and Flame (1986).
31. TSUJI, H., YAMAOKA, I.: Thirteenth Symposium (International) on Combustion, p. 729, The Combustion Institute, 1971.
32. MILLER, J.A., KEE, R.J., SMOOKE, M.D., GREAR, J.F.: The Computation of the Structure and Extinction Limit of a Methane-Air Stagnation Point Diffusion Flame, Paper WSS/CI 84-10, Western States Section of the Combustion Institute, Spring Meeting 1984.
33. PETERS, N., KEE, R.J.: The computation of stretched laminar methane-air diffusion flames using a reduced four-step mechanism, Combust. Flame, *68*, 17 (1987).
34. SESHADRI, K., PETERS, N.: Asymptotic analysis of the structure of methane-air diffusion flames using a reduced three-step mechanism, to appear in Combust. Flame (1987).

35. PETERS, N.: Twentieth Symposium (International) on Combustion, p. 353, The Combustion Institute, 1984.

36. SESHADRI, K., PURI, I., PETERS, N.: Combust. Flame *61*, 237 (1985).

37. ROGG, B., BEHRENDT, F., WARNATZ, J.: Turbulent non-premixed combustion in partially premixed diffusion flamelets with detailled chemistry, This Symposium (1986).

38. LIEW, S.K., BRAY, K.N.C., MOSS, J.B.: Combust. Flame *56*, 199 (1984).

39. LIEW, S.K., MOSS, J.B., BRAY, K.N.C.: Progress in Astronautics and Aeronautics *95*, 305 (1985).

40. STARNER, S.H., BILGER, R.W.: Combust. Flame *61*, 29 (1985).

41. DIBBLE, R.W., LONG, M.B., MASRI, A.: Two-dimensional imaging of C_2 in turbulent nonpremixed jet flames, Tenth International Colloquium on Dynamics of Explosions and Reactive Systems, Berkeley 1985.

42. KIRKPATRICK, S.: Rev. Mod. Phys. *45*, 576 (1973).

43. LAST, B.J., THOULESS, D.J.: Phys. Rev. Letts. *27*, 1719 (1971).

44. PETERS, N., WILLIAMS, F.A.: AIAA J. *21*, 423 (1983).

45. JANICKA, J., PETERS, N.: Nineteenth Symposium (International) on Combustion, p. 367, The Combustion Institute, 1982.

46. DONNERHACK, S., PETERS, N.: Combust. Sci. Technol. *41*, 101 (1984).

47. ISHIZUKA, S., TSUJI, H.: Eighteenth Symposium (International) on Combustion, p. 695, The Combustion Institute, 1981.

48. BUCKMASTER, J., PETERS, N.: Wind and Noise Generation in Laminar and Turbulent Diffusion Flames, unpublished.

49. PETERS, N., SMOOKE, M.D.: Combust. Flame *60*, 171 (1985).

50. BRAY, K.N.C.: Lecture Notes in Physics *241*, 3 (1985).

51. POPE, S.B.: Turbulent Premixed Flames, to appear in Annual Reviews in Fluid Mechanics (1986).

52. BRAY, K.N.C.: Turbulent Flows with Premixed Reactants, Turbulent Reacting Flows, P.A. Libby, F.A. Williams (Eds.), p. 115, Springer, Berlin, 1980.

53. BORGHI, R.: On the structure of turbulent premixed flames, Recent Advances in Aeronautical Science, C. Bruno, C. Casci (Eds.), Pergamon, 1984.

54. KLIMOV, A.M.: Zh. Prikl. Mekh. Tekh. Fiz. *3*, 49 (1963).

55. WILLIAMS, F.A.: A Review of Some Theoretical Considerations of Turbulent Flame Structure, AGARD Conf. Proc. *164*, p. II 1-1 (1975).

56. SABATHIER, F., BOYER, L., CLAVIN, P.: Prog. Aeronaut. Astronaut. *76*, 246 (1981).

57. BOYER, L., CLAVIN, P., SABATHIER, F.: Eighteenth Symposium (International) on Combustion, p. 104, The Combustion Institute, 1981.

58. SEARBY, G., SABATHIER, F., CLAVIN, P., BOYER, L.: Phys. Rev. Lett. *51*, 1450 (1983).

59. SEARBY, G., SABATHIER, F., MONREAL, J., CLAVIN, P., BOYER, L.: Prog. Astronautics and Aeronautics *95*, 103 (1984).

60. CLAVIN, P.: Progr. Energy Combust. Sci. *11*, 1 (1985).

61. CLAVIN, P., WILLIAMS, F.A.: J. Fluid Mech. *116*, 251 (1982).

62. CLAVIN, P., JOULIN, G.: J. Phys. Lett. *44*, L-1 (1983).

63. CLAVIN, P., GARCIA, P.: J. Méc. therm. appl. *2*, 245 (1983).

64. PELCE, P., CLAVIN, P.: J. Fluid Mech. *124*, 219 (1982).

65. SIVASHINSKY, G.I.: Acta Astronautica *3*, 889 (1976).

66. SIVASHINSKY, G.I.: Combust. Sci. Technol. *15*, 137 (1977).

67. SIVASHINSKY, G.I.: Acta Astronautica *4*, 1177 (1977).

68. SIVASHINSKY, G.I.: Acta Astronautica *6*, 569 (1979).

69. SIVASHINSKY, G.I.: A. Rev. Fluid Mech. *15*, 179 (1983).

70. BUCKMASTER, J.: Combust. Flame *26*, 151 (1976).

71. BUCKMASTER, J.: Combust. Flame *28*, 225 (1977).

72. BUCKMASTER, J.: Seventeenth Symposium (International) on Combustion, p. 835, The Combustion Institute, 1979.

73. BUCKMASTER, J.: Acta Astronautica *6*, 741 (1979).

74. BUCKMASTER, J., MIKOLAITIS, D.: Combust. Flame *47*, 191 (1982).

75. MATALON, M., MATKOWSKY, B.J.: J. Fluid Mech. *124*, 239 (1982).

76. MARGOLIS, S.B., MATKOWSKY, B.J.: Combust. Sci. Technol. *34*, 44 (1983).

77. KARLOVITZ, B., DENNISTON, D.K., KNAPPSCHAFER, D.H., WELLS, F.E.: Fourth Symposium (International) on Combustion, p. 613, The Combustion Institute, 1953.

78. MATALON, M.: Combut. Sci. Technol. *31*, 169 (1983).

79. CHUNG, S.H., LAW, C.K.: Combust. Flame *55*, 123 (1984).

80. ASHURST, W.T., PETERS, N., SMOOKE, M.D.: Combust. Sci. Technol. *53*, 339 (1987).

81. FRANKE, Ch., PETERS, N.: Untersuchung der Flammenkontur in einer stark turbulenten vorgemischten Anströmung, Kolloquium des SFB 224 "Motorische Verbrennung", RWTH Aachen, F. Pischinger (Ed.), p. 64–74, 1985.

82. NAMAZIAN, M., SHEPHERD, I.G., TALBOT, L.: Combust. Flame *64*, 299 (1986).

83. ASHURST, W.T., BARR, P.K.: Combust. Sci. Technol. *34*, 227 (1983).

84. BARITAUD, T.A., GREEN, R.M.: SAE-paper 860025 (1986).

85. ZUR LOYE, A.O., BRACCO, F.V.: International Symposium on Diagnostics and Modeling of Combustion in Reciprocating Engines, Tokyo, p. 249 (1985).

86. LIBBY, P.A., WILLIAMS, F.A.: Combust. Flame *44*, 287 (1982).

87. LIBBY, P.A., WILLIAMS, F.A.: Combust. Sci. Technol. *31*, 1 (1983).

88. LIBBY, P.A., LIÑÁN, A., WILLIAMS, F.A.: Combust. Sci. Technol. *34*, 257 (1983).

89. LIBBY, P.A., WILLIAMS, F.A.: Combust. Sci. Technol. *37*, 221 (1984).

90. DARABIHA, N., CANDEL, S.M., MARBLE, F.E.: Combust. Flame *64*, 203 (1986).

91. SATO, J., TSUJI, H.: Combust. Sci. Technol. *33*, 193 (1983).

92. SATO, J.: Nineteenth Symposium (International) on Combustion, p. 1541, The Combustion Institute, 1982.

93. SOHRAB, S.H., YE, Z.Y., LAW, C.K.: Twentieth Symposium (International) on Combustion, p. 1957, The Combustion Institute, 1984.

94. CHUNG, S.H., KIM, J.S., LAW, C.K.: Extinction of interacting premixed flames: Theory and experimental comparisons, This Symposium (1986).

95. SESHADRI, K., PETERS, N.: Combust. Sci. Technol. *83*, 35 (1983).

96. TAM, R., LUDFORD, G.S.S.: Combust. Sci. Technol. *40*, 303 (1984).

97. TAM, R., LUDFORD, G.S.S.: Combust. Sci. Technol. *43*, 227 (1985).

98. ROGG, B.: Response and flamelet structure of stretched premixed methane-air flames, to appear in Combust. Flame (1986).

99. PETERS, N., WILLIAMS, F.A.: Combust. Flame *68*, 185 (1987).

100. BRAY, K.N.C., MOSS, J.B.: Acta Astronautica *4*, 291 (1977).

101. BRAY, K.N.C., LIBBY, P.A.: Phys. Fluids *19*, 1687 (1976).

102. LIBBY, P.A., BRAY, K.N.C., MOSS, J.B.: Combust. Flame *34*, 285 (1979).

103. LIBBY, P.A., BRAY, K.N.C.: Combust. Flame *39*, 33 (1980).

104. LIBBY, P.A., BRAY, K.N.C.: AIAA J. *19*, 205 (1981).

105. BRAY, K.N.C., LIBBY, P.A., MASUYA, G.M., MOSS, J.B.: Combust. Sci. Technol. *25*, 127 (1981).

106. BRAY, K.N.C., LIBBY, P.A., MOSS, J.B.: Combust. Sci. Technol. *41*, 143 (1984).

107. BRAY, K.N.C., LIBBY, P.A., MOSS, J.B.: Twentieth Symposium (International) on Combustion, p. 421, The Combustion Institute, 1984.

108. BRAY, K.N.C., LIBBY, P.A., MOSS, J.B.: Combust. Flame *61*, 87 (1985).

109. BRAY, K.N.C., CHAMPION, M., DAVE, N., LIBBY, P.A.: Combust. Sci. Technol. *46*, 31 (1986).

110. BRAY, K.N.C.: Seventeenth Symposium (International) on Combustion, p. 223, The Combustion Institute, 1979.

111. BRAY, K.N.C., LIBBY, P.A., MOSS, J.B.: *Convective Transport and Instability Phenomena* (J. Zierep and H. Oertel, Eds.), p. 389, Braun-Verlag, Karlsruhe, 1982.

112. LIBBY, P.A.: Progr. Energy Combust. Sci. *8*, 351 (1984).

113. SHEPHERD, I.G., MOSS, J.B., BRAY, K.N.C.: Nineteenth Symposium (International) on Combustion, p. 422, The Combustion Institute, 1982.

114. SHEPHERD, I.G., MOSS, J.B.: Combust. Sci. Technol. *33*, 231 (1983).

115. GOULDIN, F.C., DANDEKAR, K.V.: AIAA J. *22*, 655 (1984).

116. GOULDIN, F.C., HALTHORE, R.N.: Rayleigh scattering for density measurements in premixed flames, to appear in Experiments in Fluids (1986).

117. ANAND, M.S., POPE, S.B.: Calculations of premixed turbulent flames by pdf methods, Spring Meeting of the Central States Section of the Combustion Institute (1986).

118. ABDEL-GAYED, R.G., BRADLEY, D.: Sixteenth Symposium (International) on Combustion, p. 1725, The Combustion Institute, 1977.

119. ABDEL-GAYED, R.G., BRADLEY, D., MCMAHON, M.: Seventeenth Symposium (International) on Combustion, p. 245, The Combustion Institute, 1979.

120. ABDEL-GAYED, R.G., BRADLEY, D.: Phil. Trans. Royal Society of London A *301*, 1 (1981).

121. ABDEL-GAYED, R.G., AL-KISHALI, K.J., BRADLEY, D.: Proc. Royal Society A *391*, 393 (1984).

122. ABDEL-GAYED, R.G., BRADLEY, D., HAMID, M.N., LAWES, M.: Twentieth Symposium (International) on Combustion, p. 505, The Combustion Institute, 1984.

123. ABDEL-GAYED, R.G., BRADLEY, D.: Combust. Flame *62*, 61 (1985).

124. ABRAHAM, J., WILLIAMS, F.A., BRACCO, F.V.: SAE-paper 850345 (1985).

125. KLIMOV, A.M.: Dokl. Akad. Nauk SSSR *221*, 56–59 (1975), Engl. Translation: Sov. Phys. Dokl. *20*, 168 (1975).

126. KLIMOV, A.M.: Prog. Aero. Astro. *88*, 133 (1983).

127. KERSTEIN, A.R.: Pair-exchange model of turbulent premixed flame propagation, This Symposium (1986).

128. GOULDIN, F.C.: An application of fractals to modeling premixed turbulent flames, Sibley

School of Engineering report, Cornell University, Ithaka, N.Y. (1986).

129. MANDELBROT, B.B.: J. Fluid Mech. *72*, 401 (1975).

130. MANDELBROT, B.B.: Lecture Notes in Math. *565*, 121 (1976).

131. MANDELBROT, B.B.: The Fractal Geometry of Nature, W.H. Freeman Co., New York, 1983.

132. DAMKÖHLER, G.: Zt. f. Elektroch. *46*, 601 (1940).

133. FRISCH, U., SULEM, P.L., NELKIN, M.: J. Fluid Mech. *87*, 719 (1978).

134. HENTSCHEL, H.G.E., PROCACCIA, I.: Physical Review A *29*, 1461 (1984).

135. CHENG, W.: Private communication (1986).